

## Hydraulic properties of Douglas-fir (*Pseudotsuga menziesii*) branches and branch halves with reference to compression wood

RACHEL SPICER and BARBARA L. GARTNER

Forest Research Laboratory, Oregon State University, Corvallis, OR 97331, USA

Received January 14, 1998

**Summary** Douglas-fir (*Pseudotsuga menziesii* var. *menziesii* (Mirb.) Franco) branch segments were used to test the hypothesis that compression wood reduces xylem transport efficiency. Whole 3-year-old segments were first measured for specific conductivity ( $k_s$ ,  $\text{m}^2 \text{s}^{-1} \text{MPa}^{-1}$ ), then split lengthwise into upper and lower halves, the latter containing all or most of the compression wood in the segment. Halves were then re-measured for  $k_s$  using a new technique that prevents leakage of permeating fluid during measurements. Lower branch halves had significantly lower  $k_s$  than upper halves ( $6.4 \pm 0.3$  versus  $9.3 \pm 0.3 \text{ m}^2 \text{ s}^{-1} \text{MPa}^{-1} \times 10^{-4}$ , respectively;  $n = 36$ ), and despite their larger size, significantly lower hydraulic conductivity ( $k_h$ ,  $\text{m}^4 \text{ s}^{-1} \text{MPa}^{-1}$ ) than upper halves. Lower branch halves had higher specific gravity ( $0.51 \pm 0.01$  versus  $0.45 \pm 0.01$ ;  $n = 36$ ), lower water content ( $123 \pm 2\%$  versus  $155 \pm 3\%$ ;  $n = 36$ ), and larger proportions of volume occupied by both cell wall and air than upper halves. Lower halves had more tracheids per annual ring than upper halves ( $73 \pm 3$  versus  $63 \pm 2$  per radial transect, respectively;  $n = 36$ ), but tracheids were shorter and had narrower lumens than those of upper branch halves. Differences in hydraulic properties between upper and lower halves suggest that compression wood does reduce xylem transport efficiency. In contrast, the amount of compression wood in each sample did not explain any variation in whole unsplit sample hydraulic properties.

**Keywords:** compression wood, hydraulic conductivity, leaf-specific conductivity, specific conductivity.

### Introduction

Xylem serves both mechanical and hydraulic functions throughout the plant stem. Unlike angiosperm xylem, in which a great variety of cell types and configurations allow for specialization, the more primitive xylem of gymnosperms consists almost entirely of tracheids (90 to 94% by volume, Panshin and de Zeeuw 1980). This single cell type must then perform both mechanical and hydraulic functions. Although it is often suggested that xylem formation represents a tradeoff between mechanical support and an efficient supply of water to the foliage, experimental evidence for such a tradeoff is mixed. Artificially supported stems require a smaller cross-sectional area of xylem per unit foliage than self-supported stems, sug-

gesting a hydraulic cost for mechanical support (Dean 1991, Gartner 1991). In contrast, age-related changes in xylem development for self-supported stems do not suggest such a tradeoff (Mencuccini et al. 1997).

Gymnosperm xylem is far from uniform despite the dominance of a single cell type, and patterns of variation in tracheid dimension result in patterns of variation in both mechanical and hydraulic properties within a single stem (Zobel and van Buijtenen 1989, Gartner 1995). One example of this variation is compression wood, which forms in gymnosperms on the undersides of branches and leaning stems as a means of mechanical support (Sinnott 1952, Westing 1965, 1968, Boyd 1973). Typical compression wood has wide annual rings and is much denser than normal wood, owing to tracheids with small lumens and thick, highly lignified cell walls that differ in ultrastructure from those of normal wood (Côté and Day 1965, Kennedy and Farrar 1965, Côté et al. 1967, Yoshizawa and Idei 1987). Compression wood tracheids are also shorter than normal wood tracheids and frequently have distorted and bifurcated tips (Siripatanadilok and Leney 1985, Yoshizawa et al. 1985b, Yoshizawa and Idei 1987, Yoshizawa et al. 1987).

Although compression wood often is considered a discrete entity, the anatomical characteristics associated with compression wood form a continuum about the circumference of a stem or branch. Thus, the wood formed directly opposite compression wood (termed “opposite wood”) typically forms narrow annual rings composed of thin-walled tracheids that are square in outline (Timell 1973, Park 1983, 1984a, 1984b, Lee and Eom 1988). Trends in tracheid length and lumen diameter are less clear (Park 1983, 1984a, 1984b), but most investigators agree that the wood formed to either side of compression wood (“lateral wood”) resembles normal wood most closely and forms an anatomical intermediate between compression and opposite wood.

Although the mechanical role of compression wood is clear (Archer and Wilson 1970, 1973, Boyd 1973, Wilson and Archer 1977), its hydraulic consequences are not. The short, small-diameter tracheids of compression wood should increase resistance to the flow of water through living trees (Bolton and Petty 1978, Calkin et al. 1986), but the anatomy of the entire shoot will determine how well the foliage is supplied with water. The wide annual rings associated with compression wood may compensate for its low permeability

by creating a larger conducting area relative to normal wood. Increased permeability of opposite or lateral wood or both could also compensate at the level of the whole shoot. Finally, the formation of three or more bands of earlywood tracheids that are normal in appearance, at the start of an annual ring containing compression wood (Core et al. 1961, Wood and Goring 1971, Yoshizawa et al. 1985a, Yoshizawa and Idei 1987), may counteract the expected hydraulic impact of compression wood.

It is surprising that among numerous studies on hydraulic architecture, the potential impact of compression wood on shoot hydraulic properties has not been addressed. In particular, long, horizontal branches may form more compression wood than short, vertical branches in order to counteract an increased downward bending moment. Increased amounts of relatively impermeable compression wood could then contribute to the observed reduction in hydraulic conductance with branch length (Waring and Silvester 1994, Panek and Waring 1995) and tree age (Ryan and Yoder 1997). In the current study, we examined the hydraulic role of compression wood in branches of young Douglas-fir trees. We first compared the hydraulic properties of upper and lower branch halves to test the hypothesis that lower branch halves conduct water less efficiently than upper branch halves. We then examined the anatomy of the branch halves to account for observed hydraulic differences. Finally, we investigated the potential for a tradeoff between hydraulic and mechanical xylem functions by relating whole-branch hydraulic properties to the amount of compression wood present in each shoot.

## Materials and methods

### Plant material

Three branches were harvested from each of 12 Douglas-fir (*Pseudotsuga menziesii* var. *menziesii* (Mirb.) Franco) trees from mid-June to early July 1995. The trees ranged in age from 8 to 12 years and were naturally regenerated, growing in an open field adjacent to Peavy Arboretum at the Oregon State University McDonald Research Forest (44°39'34" N, 123°14'01" W, 136 m elevation). Samples for conductivity measurements (one per branch) were taken from the 3-year-old portion (i.e., the third "interwhorl" from the tip) of the main axis of 5-, 6- and 7-year-old branches. Segments closest to the main stem (i.e., segments from 5-year-old branches) were expected to have more compression wood than segments closest to the branch tip (i.e., segments from 7-year-old branches). In this way, sample age, normally a strong determinant of hydraulic properties, was held constant while providing a range in the amount of compression wood in each sample.

Before branch harvest, the region to be sampled was marked and measured for its angle with respect to the vertical by lining the flat side of a protractor against the bottom of the marked region and reading the angle from a weighted string. To minimize tension in the xylem sap and reduce the risk of introducing emboli, whole branches were harvested before dawn and the cut ends immediately immersed in water for transport to the laboratory. All conductivity measurements were made on the day of branch harvest.

### Whole-branch segments

**Sample preparation** A 5-cm-long segment was excised under water from the main axis of each branch near the base of the 3-year-old portion of the shoot. The bark was removed and the ends shaved with a razor blade. The area of compression wood visible on the proximal end of each segment was traced onto acetate paper and later measured with the image analysis system described below. Segment diameter, length and pith diameter were measured with calipers. The segments remained submerged in water at room temperature until conductivity measurements were made.

**Leaf area** Foliage attached and distal to each branch segment was collected and separated into two age classes: current-year and non-current year. For each branch and age class, fresh needles were removed from five randomly selected, 4-cm-long sprigs. The remaining foliage was oven-dried at 60 °C for 48 h and then weighed. The projected area of fresh foliage samples was determined with a video camera and the NIH Image software package (Version 1.52, U.S. National Institute of Health). Area to weight ratios did not vary significantly with branch age, and samples were pooled to yield the following conversions (mean ± SE,  $n = 36$ ); the ratio of fresh area to dry weight was  $85.5 \pm 1.4 \text{ cm}^2 \text{ g}^{-1}$  for current-year foliage, and  $70.5 \pm 0.6 \text{ cm}^2 \text{ g}^{-1}$  for older foliage.

**Specific conductivity** Specific conductivity ( $k_s$ ) describes the permeability of a xylem segment following Darcy's Law and is defined as:

$$k_s = \frac{Ql}{A_s \Delta P},$$

where  $k_s$  is in  $\text{m}^2 \text{ s}^{-1} \text{ MPa}^{-1}$ ,  $Q$  is the volume flow rate ( $\text{m}^3 \text{ s}^{-1}$ ),  $l$  is the length of the segment (m),  $A_s$  is the sapwood cross-sectional area ( $\text{m}^2$ ), and  $\Delta P$  is the pressure difference between the two ends of the segment (MPa). All calculations, including hydraulic conductivity and leaf-specific conductivity (defined below), were corrected to 20 °C to account for changes in fluid viscosity with temperature.

Whole-branch segments were fit with flexible tubing, and a dilute solution of oxalic acid ( $10 \text{ mol m}^{-3}$ , filtered to  $0.22 \mu\text{m}$ ) was delivered to the distal end under a gravitational pressure head of approximately 0.01 MPa. Oxalic acid has been shown to prevent the decline in conductivity with time that is observed when using distilled water during long measurement periods (Sperry et al. 1988). The fluid was collected from the proximal end in small vials for periods of 1 min and weighed on an electronic balance. Volume flow rate was calculated as the mean of at least five collection periods.

Thermocouples were used to record the temperature of both the oxalic acid and the water in which samples were held prior to conductivity measurements to account for changes in fluid viscosity.

**Hydraulic conductivity** Hydraulic conductivity ( $k_h$ ) expresses the volume flow–pressure relationship on a sample length but not area basis, and is defined as:

$$k_h = \frac{Ql}{\Delta P},$$

where  $k_h$  is in  $\text{m}^4 \text{s}^{-1} \text{MPa}^{-1}$ .

**Leaf-specific conductivity and Huber value** Leaf-specific conductivity ( $k_l$ ) expresses conductivity per distal leaf area rather than per sapwood cross-sectional area and is defined as:

$$k_l = \frac{Ql}{A_l \Delta P},$$

where  $k_l$  is in  $\text{m}^2 \text{s}^{-1} \text{MPa}^{-1}$  and  $A_l$  is the sum of the projected leaf area both attached and distal to the segment ( $\text{m}^2$ ). Huber value (HV) is defined as the ratio of xylem cross-sectional area to distal leaf area, and is therefore unitless. Note that:

$$k_l = \text{HV}(k_s).$$

#### Branch halves

**Sample preparation** Following conductivity measurements on whole-branch segments, each segment was split lengthwise through the pith (starting at the proximal end) with a razor blade and chisel under water. In this way each segment was divided into upper and lower branch halves, the latter containing all or most of the compression wood in the segment (Figure 1). Halves were quickly surface-dried with a towel and weighed. Volume flow rates were then measured to calculate both hydraulic conductivity ( $k_h$ ) and specific conductivity ( $k_s$ ). Preliminary tests showed that volume flow rate could be measured twice on the same sample, with several hours between measurements, without significantly affecting the results.

Halves were not always equal in size because of the eccentric growth associated with compression wood and the nature of splitting wood. The former determined the size of halves at the proximal end where the samples were split directly through the pith, and the latter affected the size of halves at the distal end. Fifteen samples (30 halves) showed an appreciable difference in size, in which case the cross-sectional area of both ends was measured on thin sections with the image analysis system

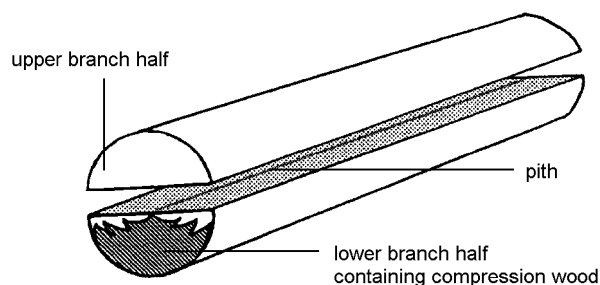


Figure 1. Branch segment split longitudinally through the pith into upper and lower halves, the latter containing all of the compression wood in the sample.

described for leaf area. Cross-sectional area was then calculated as the mean of the area of the proximal and distal ends. For the remainder of the samples (42 halves), paired halves were equal in size and cross-sectional area was calculated only for the proximal end.

**Pressure-sleeve apparatus** Branch halves were enclosed in a pressure-sleeve apparatus to seal the sides of the segments to prevent leakage during conductivity measurements. A double-ended pressure chamber (Salleo et al. 1992) was modified to house a thin latex sleeve, which, on pressurization of the air inside the chamber, was forced against the sides of the sample (Figure 2). Latex sleeves of various sizes were made from cylindrical balloons by removing the closed end with a razor blade. Perfusion of branch halves with safranin-O and tests with impermeable plastic slugs in the shape of branch halves showed that an applied air pressure of 0.1 MPa was sufficient to seal the sample sides under the range of gravitational pressure heads used here.

Branch halves were fit at both ends with tubing connectors and inserted in the pressure-sleeve apparatus. Connectors consisted of thick-walled latex tubing that fit tightly around the end of each sample and attached to a 5-cm-long section of rigid plastic tubing by layers of flexible tubing of smaller diameter. Following pressurization of the chamber to 0.1 MPa, the connectors at either end of the segment were flushed with filtered oxalic acid to remove air bubbles, then attached to the reservoir of oxalic acid (distal end), and to a 1-ml graduated pipette (proximal end). Volume flow rates were measured under the same conditions described for whole-branch segments by timing the movement of the meniscus across 0.01-ml intervals of the pipette. A mean of more than eight timed intervals was used.

Following conductivity measurements, branch halves were perfused with filtered ( $0.22 \mu\text{m}$ ), 0.5% (w/v) safranin-O for 20 min. The earlywood always stained completely giving no evidence of cavitation. Branch halves were then measured for volume by water displacement, oven-dried at  $102^\circ\text{C}$  for 48 h, and weighed.

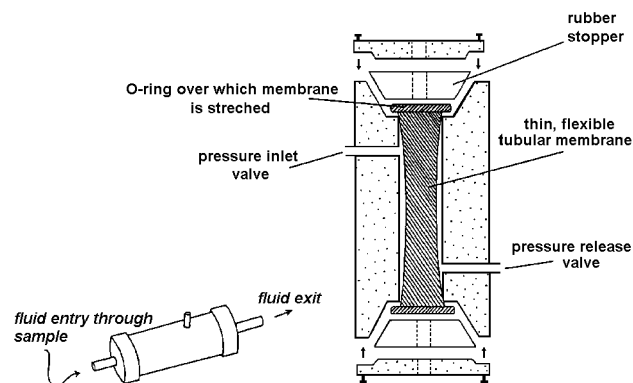


Figure 2. Pressure-sleeve apparatus. The cut radial surfaces of branch halves were sealed during volume flow rate measurements by enclosing halves within the tubular membrane and pressurizing the air inside the chamber to 0.1 MPa.

**Damage estimates** Hydraulic conductivity ( $k_h$ ) values were used to estimate the extent to which branch halves were damaged by the splitting process. For each sample, a “damage factor” (DF) was calculated as:

$$DF = \left( 1 - \frac{k_{h(\text{upper})} + k_{h(\text{lower})}}{k_{h(\text{whole sample})}} \right) 100,$$

where  $k_{h(\text{upper})}$ ,  $k_{h(\text{lower})}$ , and  $k_{h(\text{whole sample})}$  refer to upper and lower branch halves, and whole-sample (before splitting)  $k_h$ , respectively.

**Specific gravity** Specific gravity (SG) is a unitless ratio of dry weight to the weight of water displaced by a sample at a given water content and was calculated as:

$$SG = \frac{W_d}{V_f D_w},$$

where  $W_d$  is the dry weight of the segment (g),  $V_f$  is the fresh volume ( $\text{cm}^3$ ) and  $D_w$  is the density of water ( $\text{g cm}^{-3}$ ) (Siau 1984).

**Water content** Water content (WC) expresses the amount of water in wood per unit dry weight and was expressed as a percent:

$$WC = \left( \frac{W_f - W_d}{W_d} \right) 100,$$

where  $W_f$  is the fresh weight (g) of the segment.

**Volume occupied by cell wall material, water and air** For each branch half, the volume occupied by cell wall material (e.g., cellulose, hemicellulose and lignin), water and air was expressed as a percentage of sample fresh volume. The percentage of volume occupied by cell wall material ( $V_{\text{cell wall}}$ ) was calculated as:

$$V_{\text{cell wall}} = \left( \frac{W_d}{V_f 1.53} \right) 100,$$

where pure cell wall material is assumed to have a constant density of  $1.53 \text{ g cm}^{-3}$  (Siau 1984). The percent volume occupied by water ( $V_{\text{H}_2\text{O}}$ ) was calculated as:

$$V_{\text{H}_2\text{O}} = \left( \frac{(W_f - W_d) D_w}{V_f} \right) 100,$$

The percentage of volume not occupied by either cell wall material or water was assumed to be occupied by air ( $V_{\text{air}}$ ) and was calculated as:

$$V_{\text{air}} = (1 - (V_{\text{cell wall}} + V_{\text{H}_2\text{O}})) 100.$$

#### Xylem anatomy

Tracheid lengths and diameters were characterized for the second growth ring from the pith for all branch halves. An

image analysis system consisting of a compound microscope, video camera, computer and NIH Image was used to analyze both transverse sections and tracheid macerations.

**Tracheid lumen diameter** Transverse sections of the proximal end of each half were made with a microtome, stained with safranin-O, mounted and viewed with a  $40\times$  objective on a compound microscope. For the second annual ring of each branch half, lumen diameters were calculated from measured lumen areas along three radial cell files (about 200 lumens per branch half). Transverse sections were visually divided into three sectors of equal area, and one radial file was randomly selected from each.

Frequency distributions of tracheid lumen diameters were used to calculate the contribution of each class ( $2 \mu\text{m}$  increments) to total theoretical flow rate for each branch half. According to Poiseuille's law, the flow rate of fluid through a perfect capillary is proportional to the fourth power of the radius. Although there are good reasons why measured flow rate is typically much less than theoretical flow rate (e.g., tracheids are not perfect capillaries, bordered pits add resistance), we used the calculations to illustrate the potential hydraulic implications of different diameter distributions.

Typical compression wood tracheids did not appear until 12 to 15 cells from the start of the annual ring. To see if the largest, apparently normal earlywood tracheids differed in lumen size between upper and lower branch halves, we measured lumens of the first ten rows of tracheids (about 750 tracheids per branch half). Maximum lumen diameter was then calculated as the mean of the five largest earlywood tracheids measured for each branch half.

**Tracheid length** Matchstick-sized wedges were removed from random positions within the second growth ring of each branch half and macerated in Jeffrey's solution (10% nitric acid and 10% chromic acid, 1:1) for approximately 4 h (Berlyn and Miksche 1976). Macerations were rinsed, stained with safranin-O, mounted and viewed with a  $4\times$  objective on a compound microscope. Lengths were measured for 150–250 randomly selected tracheids per branch half.

#### Statistical analysis

Paired *t*-tests were used to test differences in hydraulic and anatomical parameters between branch halves. Analyses of variance (ANOVA) and covariance (ANCOVA) were used to test differences between the three branch ages with tree as a blocking factor. We used ANCOVA specifically to test for the significance of a covariate, percent compression wood, while controlling for the effect of sample diameter. All statistical procedures were conducted with Statistical Analysis Systems software (1996; SAS Inc., Cary, NC).

## Results

#### Whole-branch segments

The hydraulic parameters  $k_s$ ,  $k_h$  and  $k_l$  did not differ among the three branch ages ( $P > 0.05$ , one-way ANCOVA with diameter as a covariate and tree as a blocking factor, data not shown) and

are reported as pooled means for all 36 samples (Table 1). Compression wood occupied 18–60% of the sample cross section (Table 1), but showed no significant relationship with either the diameter or angle of whole-branch segments ( $P > 0.05$ , data not shown). Neither Huber value (Figure 3a),  $k_s$  (Figure 3b), nor  $k_l$  (data not shown) was related to percent compression wood ( $P > 0.05$ ).

#### Branch halves

Upper and lower branch halves differed significantly in both hydraulic and anatomical properties (Table 2), and differed similarly for all three branch ages ( $P > 0.05$ , one-way ANOVA with tree as blocking factor, data not shown). Lower branch halves had less than 70% of the  $k_s$  of upper branch halves, and although they tended to be larger (the cross-sectional area of lower branch halves made up  $52\% \pm 0.5$  (mean  $\pm$  SE) of total segment area), lower branch halves had consistently lower  $k_h$  values than upper branch halves (Table 2).

Lower branch halves had significantly lower water contents and higher specific gravity than upper halves (Table 2). The proportion of total sample volume occupied by both cell wall material and air was greater for lower branch halves than for upper branch halves, whereas the reverse was true for the volume occupied by water (Table 2). To prevent water loss before volume flow rate measurements, samples were stored in water and quickly surface-dried with a towel before weighing. Some water probably remained on the surface of samples and, as a result, the volume occupied by water will be overestimated for both halves, and the volume occupied by air will be underestimated. For some samples, the sum of calculated volumes of water and cell wall material was greater than the fresh sample volume, producing negative values for air volumes.

Although lower branch halves consistently had more cells within an annual ring, the cells tended to be shorter and, in the case of earlywood, smaller than cells in upper branch halves (Table 2). Within the second annual ring, the first-formed earlywood tracheids had the widest lumens for both branch halves, with means of 15 and 17  $\mu\text{m}$  for lower and upper halves, respectively (Figure 4). Mean lumen diameter of lower branch halves remained below that of upper halves for more than 70% of the annual ring width (Figure 4).

Table 1. Structural and hydraulic properties of branches and whole-branch segments. Values shown are pooled for all three branch ages ( $n = 36$ ).

	Mean $\pm$ SE	Minimum	Maximum
$k_s$ ( $\text{m}^2 \text{s}^{-1} \text{MPa}^{-1} \times 10^{-4}$ )	$8.1 \pm 0.3$	5.1	11.7
$k_h$ ( $\text{m}^4 \text{s}^{-1} \text{MPa}^{-1} \times 10^{-8}$ )	$4.3 \pm 0.3$	0.9	8.0
$k_l$ ( $\text{m}^2 \text{s}^{-1} \text{MPa}^{-1} \times 10^{-7}$ )	$1.42 \pm 0.04$	0.8	1.9
Huber value ( $\times 10^{-4}$ )	$1.77 \pm 0.04$	1.3	2.2
% Compression wood	$37 \pm 2$	18	60
Angle of segment ( $^\circ$ )	$64 \pm 2$	32	89
Diameter of segment (mm)	$8.2 \pm 0.2$	4.9	10.7
Leaf area distal to segment ( $\text{m}^2$ )	$0.30 \pm 0.02$	0.1	0.5

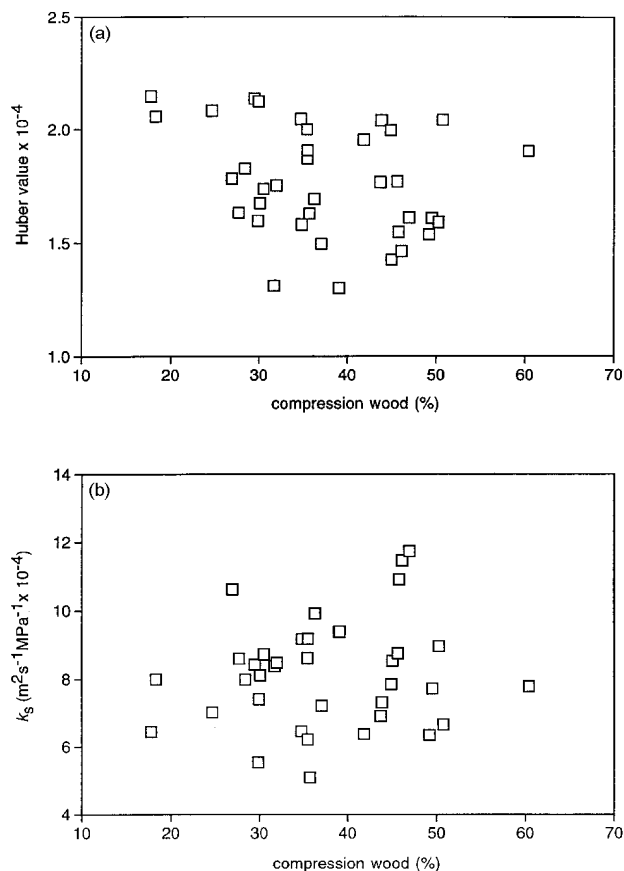


Figure 3. (a) Huber value (sapwood area:distal leaf area) and (b)  $k_s$  of whole-branch segments versus compression wood expressed as a % of sample cross-sectional area. The lack of relationship between whole-shoot hydraulic properties and % compression wood suggests there may be compensation for the low permeability of compression wood (and therefore lower branch halves) at the whole-shoot level.

Lower branch halves had a smaller range of tracheid diameters and a greater proportion of narrow tracheids than upper halves (Figure 5a). Based on calculated  $\Sigma r^4$  values, tracheids  $\geq 16 \mu\text{m}$  in diameter contributed only 29% of the total flow in lower branch halves, compared to over 60% in upper branch halves (Figure 5b). Measured differences in hydraulic conductivity between halves were slightly smaller than theoretical differences based on lumen diameter: lower branch halves had  $\Sigma r^4$  values (summed for all lumen diameter classes) that were 58% of those for upper branch halves (data not shown), whereas the measured  $k_h$  of lower branch halves was about 73% of that of upper halves (Table 2).

Damage caused by splitting, as calculated from  $k_h$  for branch halves and whole-branch segments, ranged from 0 to 36% with a mean ( $\pm$  SE) of  $12 \pm 1\%$ . The smallest diameter samples were most affected by the splitting process (Figure 6).

#### Discussion

We found strong evidence supporting the hypothesis that lower

Table 2. Hydraulic [ $k_s$  ( $\text{m}^2 \text{s}^{-1} \text{MPa}^{-1} \times 10^{-4}$ ) and  $k_h$  ( $\text{m}^4 \text{s}^{-1} \text{MPa}^{-1} \times 10^{-8}$ )] and anatomical properties of upper and lower branch halves. Means ( $\pm$  SE) are shown for all three branch ages ( $n = 36$ ).

	Upper branch half	Lower branch half	Significance <sup>1</sup>
<i>Hydraulic properties</i>			
$k_s$	9.3 $\pm$ 0.3	6.4 $\pm$ 0.3	***
$k_h$	2.2 $\pm$ 0.2	1.6 $\pm$ 0.1	**
<i>Physical properties</i>			
Specific gravity	0.45 $\pm$ 0.01	0.51 $\pm$ 0.01	***
% Water content	155 $\pm$ 3	123 $\pm$ 2	***
$V_{\text{cell wall}}$ (%)	29.0 $\pm$ 0.3	33.0 $\pm$ 0.3	***
$V_{\text{H}_2\text{O}}$ (%)	69.0 $\pm$ 0.7	62.0 $\pm$ 0.6	***
$V_{\text{air}}$ (%)	3.0 $\pm$ 0.7	5.0 $\pm$ 0.5	*
<i>Anatomical properties</i>			
Radial cell count	63 $\pm$ 2	73 $\pm$ 3	**
Maximum tracheid diameter ( $\mu\text{m}$ ) <sup>2</sup>	21.4 $\pm$ 0.4	18.6 $\pm$ 0.3	**
Tracheid length (mm)	1.40 $\pm$ 0.02	1.20 $\pm$ 0.01	**

<sup>1</sup> Significance levels are based on paired *t*-tests performed separately for each branch age ( $n = 12$ ). Asterisks indicate: \*\*\* =  $P < 0.0001$ ; \*\* =  $P < 0.001$ ; and \* =  $P < 0.01$ .

<sup>2</sup> Maximum tracheid lumen diameter for each branch half was calculated as the mean of the five largest earlywood tracheid lumens measured (a total of about 750 earlywood lumens were measured per branch half). These first-formed earlywood tracheids appeared normal, i.e., they did not exhibit cellular characteristics typical of compression wood.

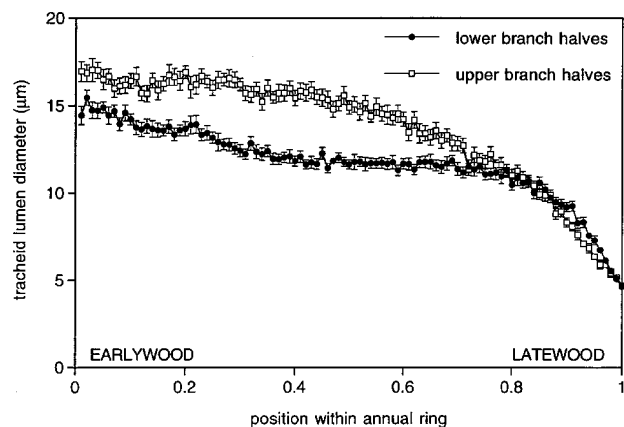


Figure 4. Trends in tracheid lumen diameter across the second annual ring for upper and lower branch halves. For each branch half, lumen diameters along three radial files were averaged by radial position. Each point represents the mean (error bars show SE;  $n$  ranged from 29 to 35 depending on how many samples had a value for that position) of the mean lumen diameter at that position for 36 branch halves.

branch halves conduct water less efficiently than upper branch halves. Two aspects of xylem anatomy could compensate for the low permeability of compression wood in the lower portion of branches to produce upper and lower halves with equal hydraulic capacity. By having a sufficient number of large

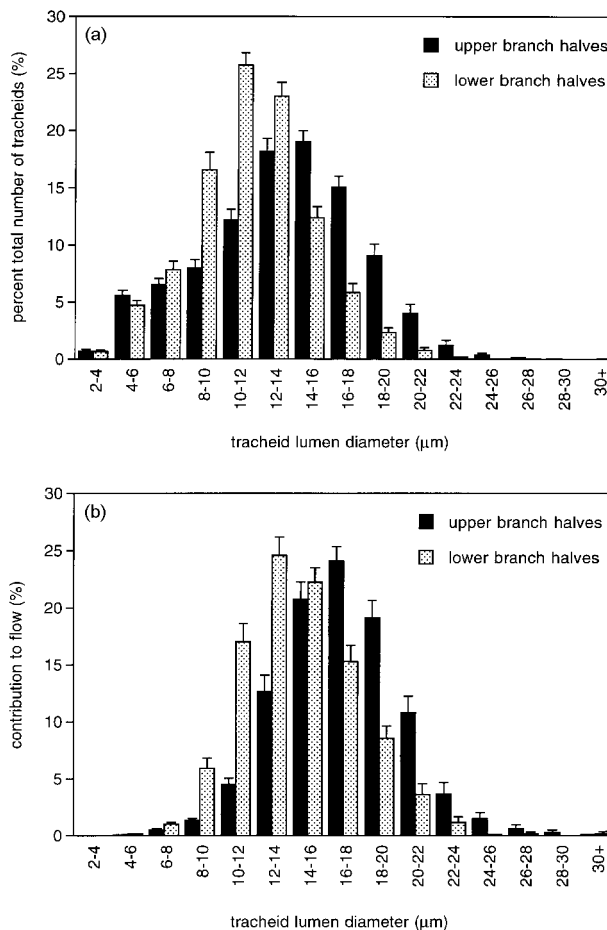


Figure 5. Frequency distributions of (a) tracheid lumen diameter and (b) the contribution of each diameter class to total theoretical flow based on  $\Sigma r^4$  values. Lower branch halves had  $\Sigma r^4$  values (summed for all lumen diameter classes) that were 58% of those for upper branch halves (data not shown). In contrast, the measured  $k_h$  of lower branch halves was about 73% of that of upper halves.

earlywood tracheids, lower branch halves could have the same  $k_s$  as upper halves. We found no evidence for this compensation, because the  $k_s$  of lower branch halves was significantly lower than that of upper halves. A larger conducting area in the lower portion of branches could also counteract the low  $k_s$  by producing upper and lower halves with equal  $k_h$  values. We found no evidence for this compensation either, suggesting that the eccentric growth associated with compression wood formation is not sufficient to compensate for its low permeability.

The low  $k_s$  of lower branch halves can be explained by their xylem anatomy. Poiseuille's law suggests that the large earlywood tracheids (or vessels in angiosperms) are responsible for most of the flow within an annual ring (Zimmermann 1983). Although we observed up to 15 rows of normal earlywood tracheids in lower branch halves, even the largest of these tracheids were significantly smaller than those of upper branch halves. This slight difference in the size of the largest cells contributes to the dramatic reduction in  $k_s$  for lower halves. For

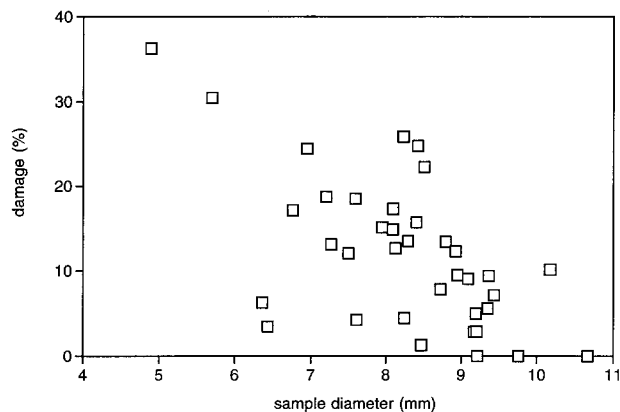


Figure 6. Damage factors as a function of sample diameter. Percent damage (DF%) was based on  $k_h$  values for branch halves relative to  $k_h$  of whole segments (see text for details).

instance, tracheids 18–20  $\mu\text{m}$  in diameter made up roughly 2.5 and 9% of all cells measured, but contributed 8 and 20% to total theoretical flow for lower and upper halves, respectively. In addition to tracheid diameter, measured differences in tracheid length between halves could explain the low  $k_s$  of lower branch halves. Water must pass through bordered pit pairs to move from tracheid to tracheid in gymnosperms and pteridophytes and this contributes significantly to the resistance to flow (Zimmermann and Brown 1971, Bolton and Petty 1978, Gibson et al. 1985, Calkin et al. 1986). Shorter tracheids found in lower branch halves would require more frequent passage through pit pairs, increasing resistance relative to upper halves. In addition to tracheary dimensions measured here, the size of pores in the bordered pit membranes, the shape of the bordered pit aperture, and the frequency of pitting should all affect resistance to flow. In well-developed compression wood, like that found in the lower portion of branches, tracheids have fewer bordered pits on their radial walls and smaller pit apertures than those of normal wood (Ohtani and Ishida 1981 (as reviewed in Timell 1986), Lee and Eom 1988).

The high specific gravity and low water content of lower branch halves result from large amounts of cell wall material relative to upper branch halves. In addition to having less overall void space (i.e., space not occupied by cell wall), lower halves had more void space occupied by air than upper halves. This could further reduce the  $k_s$  of lower branch halves if the air were to occupy tracheids (Puritch 1971, Edwards and Jarvis 1982, Pothier et al. 1989, Sellin 1991). However, we did not find any relationship between air content and  $k_s$ , suggesting that the additional air in lower branch halves may occupy the intercellular spaces found in compression wood.

Despite the reduced permeability of lower branch halves, the amount of compression wood visible on the end of each sample did not explain any variation in whole-sample hydraulic properties (i.e., it was not a significant covariate, even after the inclusion of sample diameter in the model). This lack of relationship between conductivity ( $k_1$ ,  $k_s$ , and  $k_h$ ) and percent compression wood suggests that the amount of compression wood visible in cross section is not an adequate index of its

effect on water transport. It may be that compression wood severity, rather than amount, determines the effect on hydraulics. We were not able to separate the two effects in the current study. Indices describing severity, especially those based on the large earlywood tracheids (e.g., Harris 1976), may be useful in gauging the effect of compression wood formation on the efficiency of xylem transport.

One final possibility is that the formation of opposite wood in upper branch halves compensates for lost conductive capacity due to compression wood. However, if opposite wood were to counteract the hydraulic effect of compression wood, one would expect the  $k_s$  of upper branch halves to increase and the  $k_s$  of lower branch halves to decrease with increasing percent compression wood. We did not find this to be the case.

The finding that percent compression wood was independent of both segment diameter and angle (i.e., angle of the segment within the branch, measured with respect to the vertical) underscores the complexity of compression wood formation in branches. Stems and branches have a predetermined equilibrium position (EP), such that movement out of this position stimulates compression wood formation that will return the shoot to its EP (Little 1967, Wilson and Archer 1974). In contrast to stems, for which deviation from the EP can be approximated by the angle of lean, deviation from the EP in branches is hard to assess (Timell 1986). Future work in compression wood hydraulics will require a more thorough treatment of branch mechanics in order to investigate the potential tradeoff between mechanical support and water transport functions of gymnosperm xylem. Given the importance of xylem efficiency to whole-plant productivity and the low permeability of compression wood, more research is needed to determine the integrated effect of compression, opposite and lateral woods on whole shoot water relations.

#### Acknowledgments

This research was made possible by a U.S. Environmental Protection Agency Graduate Fellowship (STAR Program) and a special grant from the U.S. Department of Agriculture for Wood Utilization Research. We are grateful to Lisa Ganio for her statistical advice, and Richard Waring and Steven Radosevich for insightful comments on an earlier draft of the manuscript.

#### References

- Archer, R.R. and B.F. Wilson. 1970. Mechanics of the compression wood response. I. Preliminary analyses. *Plant Physiol.* 46:550–556.
- Archer, R.R. and B.F. Wilson. 1973. Mechanics of the compression wood response. II. On the location, action, and distribution of compression wood formation. *Plant Physiol.* 51:777–782.
- Berlyn, G.P. and J.P. Miksche. 1976. *Botanical microtechnique and cytochemistry*. Iowa State University Press, Ames, IA, 326 p.
- Bolton, A.J. and J.A. Petty. 1978. A model describing axial flow of liquids through conifer wood. *Wood Sci. Technol.* 12:37–48.
- Boyd, J.D. 1973. Compression wood force generation and functional mechanics. *N.Z. J. For. Sci.* 3:240–258.
- Calkin, H.W., A.C. Gibson and P.S. Nobel. 1986. Biophysical model of xylem conductance in tracheids of the fern *Pteris vittata*. *J. Exp. Bot.* 37:1054–1064.

- Core, H.A., W.A. Côté, Jr. and A.C. Day. 1961. Characteristics of compression wood in some native conifers. *For. Prod. J.* 11:356–362.
- Côté, W.A., Jr. and A.C. Day. 1965. Anatomy and ultrastructure of reaction wood. *In Cellular Ultrastructure of Woody Plants*. Ed. W.A.J. Côté, Jr. Syracuse University Press, Syracuse, NY, pp 391–411.
- Côté, W.A., Jr., A.C. Day, N.P. Kutscha and T.E. Timell. 1967. Studies on compression wood. V. Nature of compression wood formed in the early springwood of conifers. *Holzforschung*. 21:180–186.
- Dean, T.J. 1991. Effect of growth rate and wind sway on the relation between mechanical and water-flow properties in slash pine seedlings. *Can. J. For. Res.* 21:1501–1506.
- Edwards, W.R.N. and P.G. Jarvis. 1982. Relations between water content, potential and permeability in stems of conifers. *Plant Cell Environ.* 5:271–277.
- Gartner, B.L. 1991. Stem hydraulic properties of vines versus shrubs of western poison oak, *Toxicodendron diversilobum*. *Oecologia* 87:180–189.
- Gartner, B.L. 1995. Patterns of variation within a tree and their hydraulic and mechanical consequences. *In Plant Stems: Physiology and Functional Morphology*. Ed. B.L. Gartner. Academic Press, New York, pp 125–149.
- Gibson, A.C., H.W. Calkin and P.S. Nobel. 1985. Hydraulic conductance and xylem structure in tracheid-bearing plants. *IAWA Bull.* 6:293–302.
- Harris, R.A. 1976. Characterization of compression wood severity in *Pinus echinata* Mill. *IAWA Bull.* 4:47–50.
- Kennedy, R.W. and J.L. Farrar. 1965. Tracheid development in tilted seedlings. *In Cellular Ultrastructure of Woody Plants*. Ed. W.A. Côté, Jr. Syracuse University Press, Syracuse, NY, pp 419–453.
- Lee, P.W. and Y.G. Eom. 1988. Anatomical comparison between compression wood and opposite wood in a branch of Korean pine (*Pinus koraiensis*). *IAWA Bull.* 9:275–284.
- Little, C.H.A. 1967. Some aspects of apical dominance in *Pinus strobus*. Ph.D. Thesis, Yale University, New Haven, CT, 234 p.
- Mencuccini, M., J. Grace and M. Fioravanti. 1997. Biomechanical and hydraulic determinants of tree structure in Scots pine: anatomical characteristics. *Tree Physiol.* 17:105–113.
- Ohtani, J. and S. Ishida. 1981. Study on the pit of wood cells using scanning electron microscopy. 6. Pits of compression wood tracheids of *Abies sachalinensis*. *Proc. Hokkaido Japanese Wood Research Soc.* 13:1–4.
- Panek, J.A. and R.H. Waring. 1995. Carbon isotope variation in Douglas-fir foliage: improving the  $\delta^{13}\text{C}$ -climate relationship. *Tree Physiol.* 14:657–663.
- Panshin, A.J. and C. de Zeeuw. 1980. *Textbook of wood technology*, 4th Edn. McGraw-Hill, New York, 722 p.
- Park, S. 1983. Structure of "opposite wood" I. Structure of the annual ring in the "opposite wood" of a horizontal growing stem of kamatsu (*Pinus densiflora* S. and Z.). *Mokuzai Gakkaishi* 29:295–301.
- Park, S. 1984a. Structure of "opposite wood" II. Variability in the diameter and wall thickness of the tracheid, ring width, and late-wood percentage. *Mokuzai Gakkaishi* 30:110–116.
- Park, S. 1984b. Structure of "opposite wood" III. Variability of the microfibril angle and length of the tracheids in peripheral positions within each annual ring including the "opposite wood." *Mokuzai Gakkaishi* 30:435–439.
- Pothier, D., H.A. Margolis, J. Poliquin and R.H. Waring. 1989. Relation between the permeability and the anatomy of jack pine sapwood with stand development. *Can. J. For. Res.* 19:1564–1570.
- Puritch, G.S. 1971. Water permeability of the wood of grand fir (*Abies grandis* (Doug.) Lindl.) in relation to infestation by the balsam woolly aphid, *Adelges piceae* (Ratz.). *J. Exp. Bot.* 22:936–945.
- Ryan, M.G. and B.J. Yoder. 1997. Hydraulic limits to tree height and tree growth. *Bioscience* 47:235–242.
- Salleo, S., T.M. Hinckley, S.B. Kikuta, M.A. Lo Gullo, P. Weilgony, T.-M. Yoon and H. Richter. 1992. A method for introducing xylem emboli *in situ*: experiments with a field-grown tree. *Plant Cell Environ.* 15:491–497.
- Sellin, A.A. 1991. Hydraulic conductivity of xylem depending on water saturation level in Norway spruce (*Picea abies* (L.) Karst.). *J. Plant Physiol.* 138:466–469.
- Siau, J.F. 1984. *Transport processes in wood*. Springer-Verlag, New York, 245 p.
- Sinnott, E.W. 1952. Reaction wood and regulation of tree form. *Am. J. Bot.* 39:69–78.
- Siripatanadilok, S. and L. Leney. 1985. Compression wood in western hemlock *Tsuga heterophylla* (Raf.) Sarg. *Wood Fiber Sci.* 17:254–265.
- Sperry, J.S., J.R. Donnelly and M.T. Tyree. 1988. A method for measuring hydraulic conductivity and embolism in xylem. *Plant Cell Environ.* 11:35–40.
- Timell, T.E. 1973. Studies on opposite wood in conifers. Part II: Histology and ultrastructure. *Wood Sci. Technol.* 7:79–91.
- Timell, T.E. 1986. *Compression wood in gymnosperms*. Vol. 1–3. Springer-Verlag, Berlin, 2150 p.
- Waring, R.H. and W.B. Silvester. 1994. Variation in foliar  $\delta^{13}\text{C}$  values within crowns of *Pinus radiata* trees. *Tree Physiol.* 14:1203–1213.
- Westing, A.H. 1965. Formation and function of compression wood in gymnosperms. *Bot. Rev.* 31:381–480.
- Westing, A.H. 1968. Formation and function of compression wood in gymnosperms. II. *Bot. Rev.* 34:51–78.
- Wilson, B.F. and R.R. Archer. 1974. Mechanical aspects of regulation of branch growth in *Pinus strobus* L. *In Mechanisms of Regulation of Plant Growth*. Eds. R.L. Bielecki, A.R. Ferguson and M.M. Creswell. *Roy. Soc. N.Z. Bull.* 12:631–636.
- Wilson, B.F. and R.R. Archer. 1977. Reaction wood: induction and mechanical action. *Annu. Rev. Plant Physiol.* 28:23–43.
- Wood, J.R. and D.A. Goring. 1971. The distribution of lignin in stem wood and branch wood of Douglas-fir. *Pulp Pap. Mag. Can.* 72:T95–T102.
- Yoshizawa, N. and T. Idei. 1987. Some structural and evolutionary aspects of compression wood tracheids. *Wood Fiber Sci.* 19:343–352.
- Yoshizawa, N., S. Koike and T. Idei. 1985a. Formation and structure of compression wood tracheids induced by repeated inclination in *Taxus cuspidata*. *Mokuzai Gakkaishi* 31:325–333.
- Yoshizawa, N., S. Matsumoto and T. Idei. 1985b. Morphological features of tracheid tips associated with compression wood formation in *Larix leptolepis* Gord. *IAWA Bull.* 6:245–253.
- Yoshizawa, N., M. Kiyomiya and T. Idei. 1987. Variations in tracheid length and morphological changes in tracheid tips associated with the development of compression wood. *Wood Sci. Technol.* 21:1–10.
- Zimmermann, M.H. 1983. *Xylem transport and the ascent of sap*. Springer-Verlag, Berlin, 143 p.
- Zimmermann, M.H. and C.L. Brown. 1971. *Trees: structure and function*. Springer-Verlag, New York, 336 p.
- Zobel, B.H. and J.P. van Buijtenen. 1989. Variation among and within trees. *In Wood Variation: Its Causes and Control*. Springer-Verlag, New York, pp 72–131.